Korean Circ J. 2020 Mar;50(3):185-202
https://doi.org/10.4070/kcj.2019.0315
pISSN 1738-5520·eISSN 1738-5555

kcj
Korean Circulation Journal

Review Article

Check for updates

Future Directions in Coronary CT Angiography: CT-Fractional Flow Reserve, Plaque Vulnerability, and Quantitative Plaque Assessment

Fernando Uliana Kay, MD, PhD, Arzu Canan, MD, and Suhny Abbara, MD

Department of Radiology, UT Southwestern Medical Center, Dallas, TX, USA.

OPEN ACCESS

Received: Sep 24, 2019
Accepted: Oct 8, 2019

Correspondence to
Fernando Uliana Kay, MD, PhD
Department of Radiology, UT Southwestern Medical Center, 5323 Harry Hines Blvd, Dallas, TX 75390, USA.
E-mail: fernando.kay@utsouthwestern.edu

ORCID iDs
Fernando Uliana Kay
https://orcid.org/0000-0002-9467-2013
Arzu Canan
https://orcid.org/0000-0002-3303-8318
Suhny Abbara
https://orcid.org/0000-0003-2552-7362

Conflict of Interest
Dr. Abbara reports personal fees from Elsevier, outside the submitted work; and Past President Society of Cardiovascular Computed Tomography (SCCT), Past President Certification Board of Cardiovascular Computed Tomography (CBCCT), Editor in Chief Radiology: Cardiothoracic Imaging. The other authors have no financial conflicts of interest.

ABSTRACT

Coronary computed tomography angiography (CCTA) is a well-validated and noninvasive imaging modality for the assessment of coronary artery disease (CAD) in patients with stable ischemic heart disease and acute coronary syndromes (ACSs). CCTA not only delineates the anatomy of the heart and coronary arteries in detail, but also allows for intra- and extraluminal imaging of coronary arteries. Emerging technologies have promoted new CCTA applications, resulting in a comprehensive assessment of coronary plaques and their clinical significance. The application of computational fluid dynamics to CCTA resulted in a robust tool for noninvasive assessment of coronary blood flow hemodynamics and determination of hemodynamically significant stenosis. Detailed evaluation of plaque morphology and identification of high-risk plaque features by CCTA have been confirmed as predictors of future outcomes, identifying patients at risk for ACSs. With quantitative coronary plaque assessment, the progression of the CAD or the response to therapy could be monitored by CCTA. The aim of this article is to review the future directions of emerging applications in CCTA, such as computed tomography (CT)-fractional flow reserve, imaging of vulnerable plaque features, and quantitative plaque imaging. We will also briefly discuss novel methods appearing in the coronary imaging scenario, such as machine learning, radiomics, and spectral CT.

Keywords: Coronary computed tomography angiography; Coronary plaque; Fractional flow reserve; Plaque characterization; Plaque volume

INTRODUCTION

After many years of diligent scientific testing and validation, coronary computed tomography angiography (CCTA) has become an established method for assessing coronary artery disease (CAD) in patients with suspected stable ischemic heart disease[1-6] and acute coronary syndrome (ACS).[7-9] Though the great legacy of earlier validation studies relies on the comparison of CCTA against reference standards, such as invasive coronary angiography (ICA), more recently, the inherent characteristics of CCTA, including 3-dimensional (3D) anatomic data and both intraluminal and extraluminal imaging, naturally allowed the emergence of newer applications in noninvasive cardiac imaging. Computational fluid dynamics (CFD) applied to CCTA have proven value in the noninvasive determination of

Author Contributions

Conceptualization: Kay FU, Canan A, Abbara S; Data curation: Canan A; Supervision: Abbara S; Writing - original draft: Kay FU; Writing - review & editing: Canan A, Abbara S.

coronary blood flow hemodynamics,[10] while plaque imaging has uncovered a multitude of imaging biomarkers capable of defining the disease stage and predicting future outcomes. Therefore, cardiac imaging research has shifted throughout the years from a luminography perspective towards a more comprehensive utilization of CCTA data. This trend has been also recently boosted by the emergence of advanced computational methods, including machine learning and artificial intelligence.[11]

In this paper, we will review the growing role of CCTA in the noninvasive assessment of myocardial ischemia using computed tomography (CT)-derived fractional flow reserve (CT-FFR). We will also review the current directions in noninvasive coronary atherosclerotic plaque imaging, focusing on the research leading to the establishment of features associated with plaque vulnerability currently used in clinical practice, as well as discussing future perspectives in quantitative coronary atherosclerotic plaque assessment. Lastly, we will present examples of emerging technology and alternative imaging biomarkers that may drive future research in CCTA.

FRACTIONAL FLOW RESERVE ASSESSED BY COMPUTED TOMOGRAPHY

Fractional flow reserve (FFR) is an invasive parameter that can be obtained during coronary angiography (invasive coronary angiography-derived fractional flow reserve [ICA-FFR]) for assessing the hemodynamic significance of stenotic lesions, which is calculated as the ratio between blood flow after a stenotic lesion and the maximum normal blood flow during myocardial hyperemia.[12] Robust data from the FFR versus Angiography for Multivessel Evaluation (FAME) study showed that ICA-FFR may be a better parameter for guiding coronary revascularization than standard angiographic interpretation. The FAME study was a randomized trial involving 20 medical centers in Europe and the United States, which compared the composite endpoint including death, nonfatal myocardial infarction, and repeat vascularization of patients selected for percutaneous implantation (percutaneous coronary intervention [PCI]) of drug-eluting stents, with 2 intervention arms adjudicated either by angiography alone or by demonstration of FFR-proven ischemia (i.e., ICA-FFR ≤0.80).[13] In this study, the event rates were determined to be 18% vs. 13% (p=0.02) for the angiography vs. FFR-guided PCI strategy in the first year of follow-up,[14] respectively, and 13% vs. 8% (p=0.02) by the end of the second year.[15] A sub-analysis of the data also found that 35% of the lesions graded with 50% to 70% of stenosis by visual angiographic assessment were actually found to be hemodynamically significant on ICA-FFR, while 20% of those graded with 71% to 90% of stenosis were deemed non-hemodynamically significant on ICA-FFR.[16] In an economic analysis of the FAME study data, not only did the FFR-guided strategy for PCI lead to an increase in quality-adjusted life-years, but also to a significant decrease in healthcare costs.[17]

CCTA is an established method capable of providing tridimensional (3D) anatomical visualization of the coronary arteries. Multiple prospective multicenter trials using 64-row multidetector scanner showed that CCTA has high sensitivity and specificity ranging from 85% to 99% and 64% to 90%, respectively, for detecting coronary stenosis of 50% or more determined by conventional angiography in cohorts of patients with suspected CAD.[18-20] However, it was shown that quantitative luminal assessment by CCTA and ICA have only weak correlation with ICA-FFR (r=−0.32 and r=−0.30), respectively.[21] More recently, CFD methods

https://doi.org/10.4070/kcj.2019.0315

have been introduced in noninvasive coronary imaging, with the goal of determining the hemodynamic significance of stenotic lesions.[22] In summary, the precursor method introducing CFD for coronary hemodynamics analysis consists of 3 steps: 1) 3D modeling of the coronary tree anatomy based on standard CCTA data, 2) defining the boundary conditions for cardiac output, aortic pressure, and myocardial microvascular resistance, and 3) solving the Navier-Stokes equations for estimation of blood flow conditions within the 3D model.[23-25] In an initial study (Diagnosis of Ischemia-Causing Stenoses Obtained Via Noninvasive Fractional Flow Reserve [DISCOVER-FLOW]), FFR was estimated from CFD modeling in 158 vessels from 103 patients concurrently undergoing CCTA (CT-FFR) and ICA-FFR at 4 centers (**Figures 1** and **2**). In this investigation, CT-FFR predicted a per-vessel ICA-FFR ≤0.80 with an accuracy of 84.3%, sensitivity of 87.9%, and specificity of 82.2%; in contrast, standard CCTA interpretation (i.e., stenosis ≥50% by visual analysis) had an accuracy of 58.5%, sensitivity of 91.4%, and specificity of 39.6%. The area under the receiver-operator characteristics curve (AUC) for detecting ICA-FFR ≤0.80 was significantly higher in CT-FFR when compared with standard CCTA interpretation (0.90 vs. 0.75, p=0.001).[10]

In a subsequent larger study (Determination of Fractional Flow Reserve by Anatomic Computed Tomographic Angiography [DeFACTO]), including 252 stable patients with suspected or known CAD from 17 centers in 5 countries, the investigators confirmed the incremental diagnostic performance of CT-FFR over CCTA alone for detecting obstructive

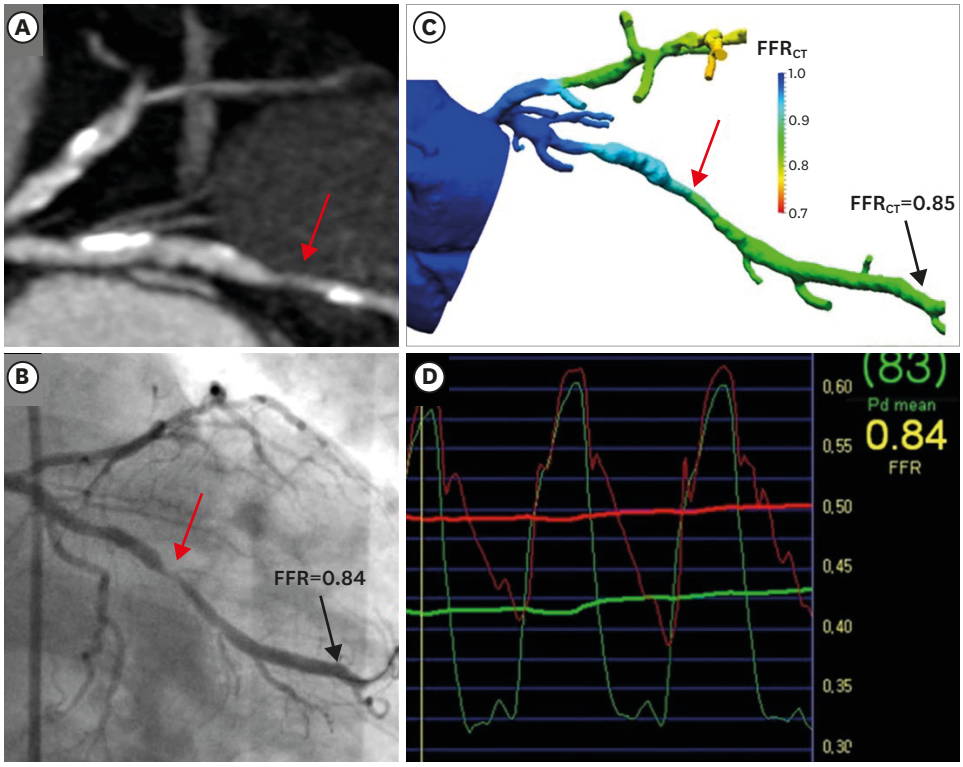

Figure 1. Stenosis without ischemia. (A) Coronary computed tomography angiography with stenosis graded >50% (arrow) in the obtuse marginal branch of the left circumflex artery. Multiple calcified plaques with stenosis between 40% and 69% are noted proximally and distally to the lesion. (B) Severe stenosis is confirmed on ICA (arrow). (C) FFR_{CT} shows a value of 0.85. (D) A reference value of 0.84 was confirmed on ICA-fractional flow reserve. Reused with permission from *J Am Coll Cardiol* 2011;58:1989-97.[10]
FFR = fractional flow reserve; FFR_{CT} = fractional flow reserve derived from coronary computed tomographic angiography data; ICA = invasive coronary angiography.

https://doi.org/10.4070/kcj.2019.0315

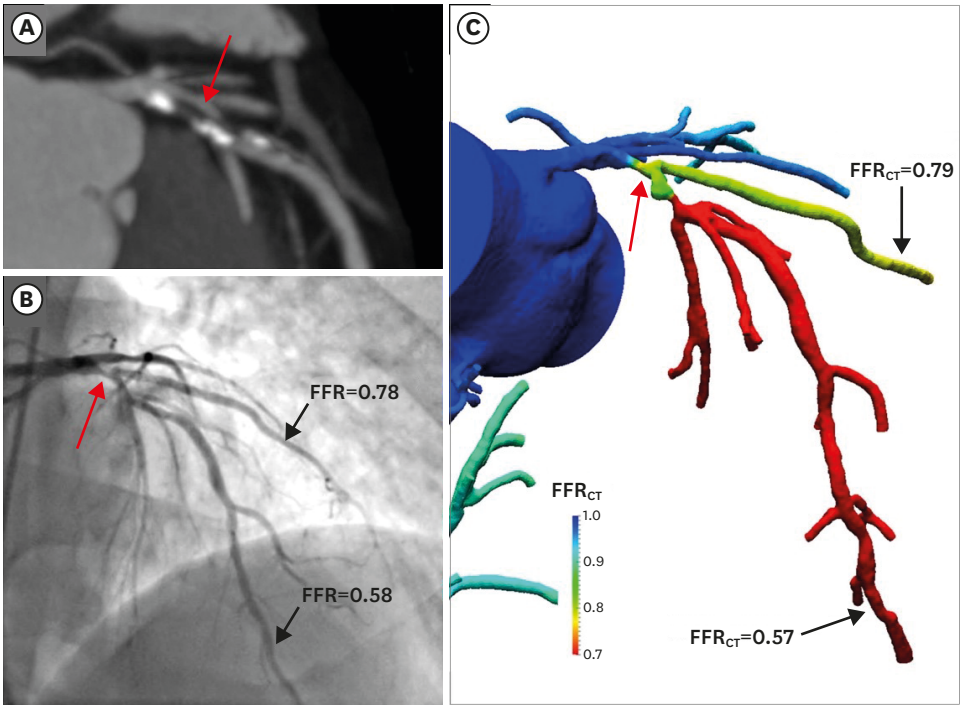

Figure 2. Stenosis with ischemia. (A) Lesion graded with >50% stenosis in the proximal LAD on multiplanar reformat of coronary computed tomography angiography (arrow). (B) Invasive coronary angiography showing the stenosis (arrow) with the corresponding reductions in coronary FFR in the first diagonal branch (FFR=0.78) and distal LAD (FFR=0.58). (C) FFR_{CT} of the first diagonal branch (0.79) and distal LAD (0.57) were determined to be 0.78 and 0.58 by computational fluid dynamics. Reused with permission from *J Am Coll Cardiol* 2011;58:1989-97.[10] FFR = fractional flow reserve; FFR_{CT} = fractional flow reserve derived from coronary computed tomographic angiography data; LAD = left anterior descending artery.

CAD as determined by ICA-FFR (AUC of 0.81 vs. 0.68, respectively, p<0.001).[26] In another multicenter study (Analysis of Coronary Blood Flow Using CT Angiography: Next Steps [NXT]), including 254 patients with suspected stable CAD, CT-FFR showed specificity of 79% to diagnose significant ischemia on a per-patient basis, which was significantly superior to CCTA (34%, p<0.001) and statistically similar to standard quantitative analysis of ICA (83%, p=0.29).[27] This study also revealed good correlation between CT-FFR and invasive ICA-FFR (Pearson's R=0.82; p<0.001), with slight underestimation of ICA-FFR by CT (difference of 0.03±0.07, mean±standard deviation).[27] Determination of CT-FFR using the aforementioned technique requires intensive post processing using parallel supercomputing capabilities from a remote core lab service,[10][26][27] which has become approved for clinical use in several countries. More recently, on-site approaches for CT-FFR analysis using modified algorithms have also emerged.[28-32]

Computed tomography-derived fractional flow reserve versus myocardial perfusion

In a prospective head-to-head comparison in 208 patients undergoing CCTA, single photon emission computed tomography (SPECT), and [^{15}O]H_2O positron emission tomography (PET) (Prospective Comparison of Cardiac PET/CT, SPECT/CT Perfusion Imaging and CT Coronary Angiography With Invasive Coronary Angiography; PACIFIC study), CT-FFR analysis could be successfully performed in 83% of the vessels (505/612); when only considering these vessels, CT-FFR showed a significantly larger AUC (0.92) for identifying ICA-FFR ≤0.80 when compared with SPECT (AUC 0.70; p<0.01) and PET (AUC 0.87; p<0.01); however, in the

https://doi.org/10.4070/kcj.2019.0315

intention-to-diagnose analysis, PET outperformed CT-FFR on a per-patient basis (AUC 0.90 vs. 0.79; p=0.005, respectively), but not on a per-vessel basis (AUC 0.86 vs. 0.83; p=0.157, respectively). In another prospective head-to-head comparison in 147 symptomatic patients referred for ICA-FFR (PERfusion Versus Fractional Flow Reserve CT Derived In Suspected CoroNary; PERFECTION study), "resting" CCTA with CT-FFR and "stress" computed tomography perfusion (CTP) were directly compared. Both CT-FFR and CTP outperformed CCTA alone on a per-vessel (accuracies of 92% and 94% vs. 82%, both p<0.001, respectively) and on a per-patient basis (accuracies of 87% and 92% vs. 73%, p= 0.001 and p<0.001, respectively), while there were no statistically significant differences between CT-FFR and CTP. Another more recent study including a smaller sample of 85 patients referred for ICA-FFR scanned in a whole-heart coverage CT scanner revealed that the combination of CCTA, CT-FFR, and CTP may outperform either one of the individual methods (AUC 0.92; p<0.05), while maintaining reasonable radiation dose (average effective dose of approximately 8 mSv for the combination of CCTA and CTP).[33] A smaller study including 37 patients undergoing perfusion cardiac magnetic resonance perfusion (CMR-P) and CT-FFR also showed correlation between ICA-FFR and a CMR-P for areas of myocardium distal to stenoses between 40% and 70% (r=−0.63; p<0.001), which was comparable to the correlation found between ICA-FFR and CT-FFR (r=0.675; p<0.001).

Computed tomography-derived fractional flow reserve versus clinical outcomes

Some studies have explored how CT-FFR may hold promise to improve clinical outcomes. The "Prospective Longitudinal Trial of FFRCT: Outcome and Resource iMpacts" (PLATFORM) study was a randomized trial including 584 patients from 11 centers, where the investigators tested the outcomes of employing CCTA with CT-FFR compared with standard non-invasive testing (i.e., any form of stress testing or CCTA without CT-FFR) in patients with new onset chest pain. They found that CT-FFR could reduce the number of diagnostic ICA with non-obstructive disease from 73% to 12% (p<0.001) at comparable cumulative radiation doses,[34] while reducing resource utilization/costs and improving quality of life.[35] Using "real-world" data from the ADVANCE registry, which included 5,083 patients, investigators have recently shown that CT-FFR may modify patient management in up to 70% of the cases (95% confidence interval [CI], 65–78%) when compared to CCTA alone.[36]

PLAQUE VULNERABILITY

One of the intrinsic technical advantages of CCTA over ICA is allowing direct atherosclerotic plaque assessment without the need for invasive transcatheter methods such as intravascular ultrasound (IVUS) or optical coherence tomography (OCT) (**Figure 3**). In fact, coronary angiography can significantly underestimate atherosclerotic plaque burden, as compensatory mechanisms are known to conserve relatively stable luminal areas even when atherosclerotic plaques involve up to 40% of the total cross-section area of the vessel, known as the positive remodeling (PR) phenomenon (**Figure 4**).[37]

Vulnerable plaques are defined as those at risk for thrombosis secondary to rupture or erosion.[38] Although the degree of stenosis increases the risk for plaque instability, the majority of the culprit lesions found in ACSs are deemed to be nonobstructive prior to rupture.[39]

Plaque characterization is an evolving field in cardiac CTA, built upon extensive knowledge derived from histopathologic studies.[40] Early CCTA studies focusing on plaque

https://doi.org/10.4070/kcj.2019.0315

kcj
Korean Circulation Journal

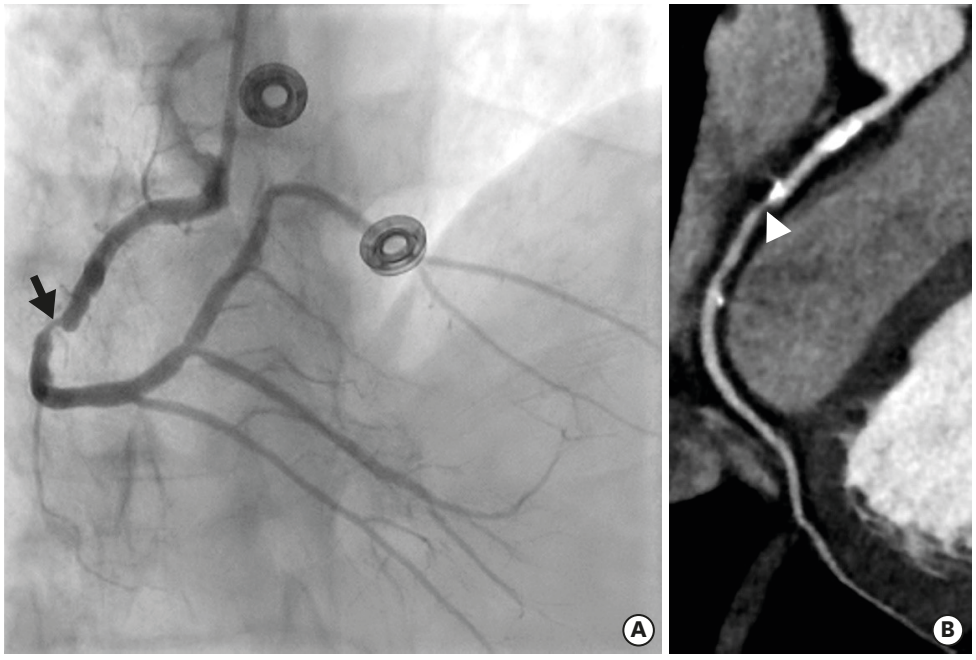

Figure 3. Direct plaque assessment. (A) Invasive coronary angiography, catheterization of the RCA. Severe stenosis of the mid RCA (arrow). (B) Coronary CT angiography, curved multiplanar reconstruction of the RCA. CT reveals a predominantly noncalcified component (arrowhead) in the obstructive mid RCA plaque. The additional calcified plaques do not cause significantly stenosis.
CT = computed tomography; RCA = right coronary artery.

Figure 4. Positive remodeling. Coronary computed tomography angiography, curved multiplanar reconstruction of the left anterior descending artery showing a predominantly noncalcified plaque in the proximal segment causing stenosis between 50% and 69%. Note the increased diameter of the vessel at the level of the stenosis (arrowheads) when compared to the segments immediately before and after the stenosis (i.e., remodeling index >1.1).

characterization identified PR as a high-risk feature. In a cross-sectional study, of 40 lesions in 14 patients with ACS and 9 patients with stable angina (SA), Hoffman et al.[41] measured the ratio between the total transverse area across the site of maximum luminal narrowing and the

https://doi.org/10.4070/kcj.2019.0315

mean areas across proximal and distal reference sites (i.e., remodeling index). They observed an increase in the remodeling index in culprit plaques in ACS patients when compared with stable plaques in ACS and SA patients (respective remodeling indexes of 1.4±0.4 vs. 1.0±0.4 vs. 1.2±0.3, p=0.04, mean±standard deviation).

In addition to PR, the histopathologic study of coronary arteries has also shown common characteristics in ruptured plaques, such as large necrotic cores and a thin fibrous caps.[40] For instance, in a histopathologic study designed to understand targetable biomarkers of vulnerable atherosclerotic plaques for invasive and noninvasive imaging, Narula et al.[42] analyzed 295 coronary lesions including stable, vulnerable, and disrupted plaques. Atherosclerotic fibrous cap thickness was determined to be the best discriminatory feature for identifying the vulnerable plaques. On CCTA, the "napkin ring" has been proposed as a noninvasive way of assessing for thin-cap fibroatheromas with CCTA.[43] This sign consists of a low-attenuation plaque core surrounded by a thin hyperattenuating ring (**Figure 5**). Although the histopathologic substrate of the napkin ring sign is still debatable, its genesis is attributed to the contrasting CT numbers between the fibrous capsular component of the plaque and its necrotic central core.[44] In a longitudinal study including 895 patients, the hazard ratio (HR) for future ACS was 5.55 (95% CI, 2.1–14.7; p<0.001) in patients with plaques displaying the napkin ring sign, which was an independent predictor even when compared with other high-risk plaque features.[45]

However, given the small magnitude of linear measurements involved in fibrous cap thickness assessment (e.g., 54–84 μm), which are significantly below the nominal spatial resolution of the current generation of clinical CT scanners, direct imaging is theoretically limited to the realm of high-resolution methods, such as transcatheter OCT.[46] In a sub-analysis of Narula and collaborators' histopathologic study[42] excluding fibrous cap thickness, macrophage infiltration and necrotic core size were identified as the most important biomarkers for plaque rupture. While macrophage infiltration and plaque inflammation have become natural targets for 18F-fluorodeoxyglucose ([^{18}F]FDG) PET[47-50] and epicardial fat imaging,[51] necrotic core has been considered a natural target for CCTA assessment. Data from CCTA using submillimeter slice thickness compared with IVUS have shown that values less than 30 Hounsfield units (HU) could be used to differentiate the coronary plaques with a "soft" lipid rich core from those with a fibrous core (**Figure 6**).[52]

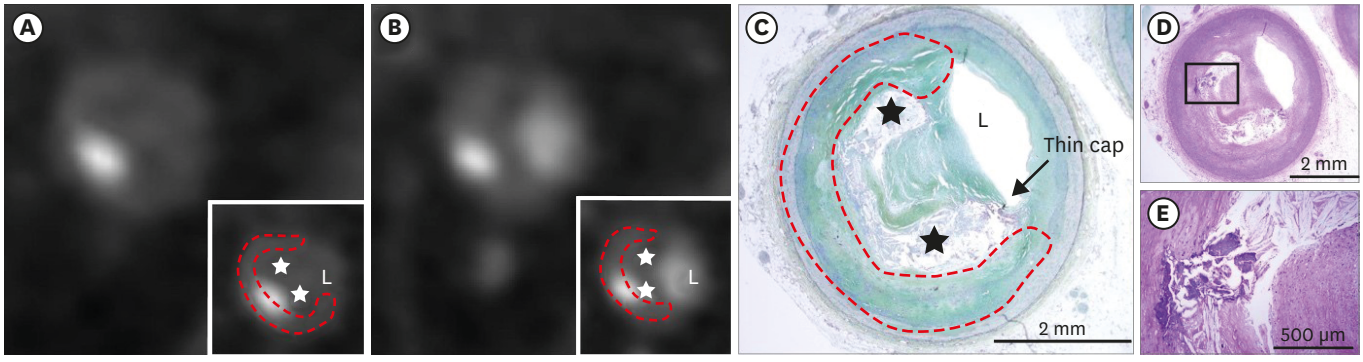

Figure 5. Napkin ring sign and spotty calcifications. Cross-sectional imaging of coronary atherosclerotic plaque showing higher computed tomography attenuation numbers within the circumferential outer rim (red dashed line) in both the noncontrast (A) and contrast-enhanced (B) images as compared to the attenuation within the central plaque (stars). Correlation with histopathology showed a thin cap fibroatheroma (C, D) with spotty calcification (E), and a necrotic core representing the low attenuation plaque core (stars in C). Fibrous plaque tissue corresponded to the hyperattenuating component within the outer rim (red dashed line). Reused with permission from *JACC Cardiovasc Imaging* 2010;3:440-4.[44]

https://doi.org/10.4070/kcj.2019.0315

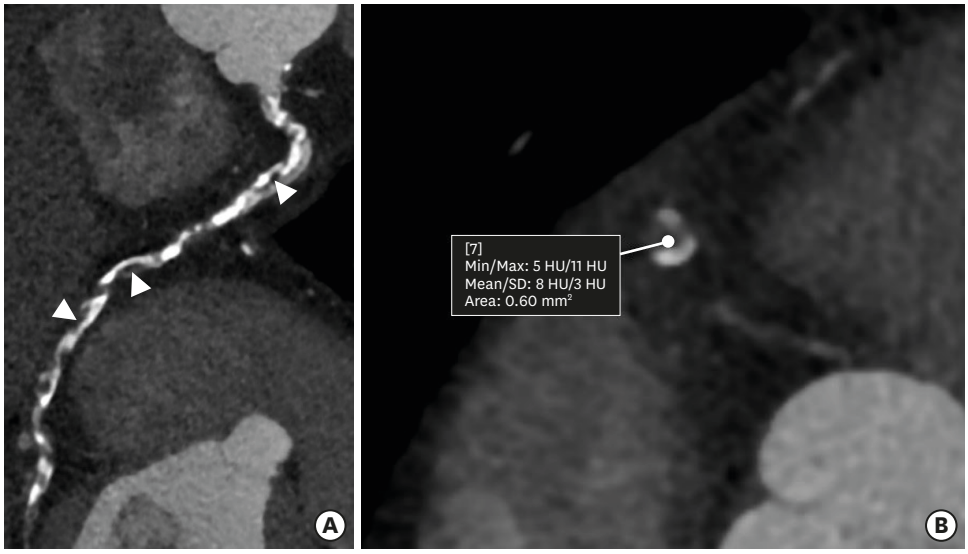

Figure 6. Low-attenuation plaque core. (A) Curved multiplanar reconstruction showing extensive atherosclerosis in the RCA, with plaques showing low-attenuation core (arrowheads). (B) Region of interest drawn in the core of the proximal RCA plaque shows a mean attenuation value of 8 HU.
HU = Hounsfield units; RCA = right coronary artery.

In a subsequent study, Motoyama et al.[53] investigated the prevalence several CCTA plaque features encountered in patients presenting with ACS and SA. They focused on features including PR, defined as a 10% increment in diameter at the plaque region when compared to a normal reference segment, and plaque consistency. The latter is subdivided based on the presence of calcifications (attenuation >220 HU) and their size (<3 mm in size defined as "spotty" vs. "large"). Noncalcified plaques were further subdivided into those with core attenuation <30 HU ("low-attenuation" core [LAC]) or between 30 HU and 150 HU. They found that PR, LAC, and spotty calcification were significantly more prevalent in ACS than SA (87% vs. 12%, p<0.001; 79% vs. 9%, p<0.001; and 63% vs. 21%, p=0.0005, respectively). In contrast, large calcifications were found more frequently in SA than ACS (55% vs. 22%, p=0.004).[53] Other studies have further confirmed the value of these high-risk plaque features for determining future ACS. In a longitudinal study including 1,059 patients imaged with CCTA, Motoyama et al.[54] found that PR or LAC (alone or in combination) were independent predictors of future ACS within a 12–50 months follow-up, with a HR of 22.8 (95% CI, 6.9–75.2; p<0.001) when compared with patients displaying neither one of these features on CCTA; these findings were subsequently confirmed by the same group in a larger cohort of 3,158 patients followed for 3.9±2.4 years.[55] In the CCTA arm of Rule Out Myocardial Ischemia/Infarction by Computer Assisted Tomography (ROMICAT) II trial,[7] high-risk features were also predictors of ACS in patients presenting to the emergency department with acute chest pain, independent of presence of obstructive CAD and clinical risk assessment.[56]

More recent analyses of large longitudinal multicenter trials have also confirmed the role of high-risk plaque features in predicting adverse major cardiovascular events. In a sub-analysis of the Prospective Multicenter Imaging Study for Evaluation of Chest Pain (PROMISE) trial,[5] investigators studied if CCTA features of high-risk plaque ("vulnerable") and significant stenosis could predict a composite endpoint including death, myocardial infarction, or SA in the 4,415 patients undergoing CCTA. Vulnerable plaques were associated with higher event rates (HR, 2.73; 95% CI, 1.89–3.93), even after adjustments for ASCVD risk score and

https://doi.org/10.4070/kcj.2019.0315

significant stenosis (HR, 1.72; 95% CI, 1.13–2.62).[57] In a post hoc analysis of the Scottish Computed Tomography of the HEART Trial (SCOT-HEART), the investigators found a HR of 3.01 (95% CI, 1.61–5.63; p=0.001) for a composite endpoint of coronary heart disease death or nonfatal myocardial infarction in patients with at least one adverse plaque feature when compared with those without any.[58]

As a result of the robust evidence for high-risk plaque features available in the literature, guidelines on CCTA reporting available on the Coronary Artery Disease Reporting & Data System (CAD-RADS™) have included a descriptor for vulnerability ("V" modifier), which is based on the presence of at least 2 of the following findings: PR, low attenuation, spotty calcification, or napkin ring.[59] In a study determining the inter-observer agreement of CAD-RADS™ lexicon including 50 CCTA with 8% prevalence of high-risk plaque features ("V"), Fleiss' Kappa for spotty calcification, napkin ring sign, PR, and low attenuation plaque were 0.29 (p<0.001), 0.15 (p=0.013), 0.34 (p<0.001), and 0.24 (p<0.001).[60] As a future perspective, more objective assessment methods could be developed to improve the slight to fair inter-observer agreement currently observed.

QUANTITATIVE PLAQUE ASSESSMENT

More recently, efforts have been made to extract quantifiable and reproducible features from digital medical imaging, known as quantitative imaging biomarkers.[61] These features can be used to diagnose disease, determine severity, and monitor progression or response to therapy. Coronary calcium scoring using the Agatston method is the precursor quantitative imaging biomarker in cardiac CT.[62] Nowadays, technological advances have recently allowed semi-automatically our automatically imaging analysis, decreasing post processing times and improving inter-observer variability.[63] These quantitative tools for coronary plaque assessment on CCTA that emerged in the last decade[64][65] have the potential to leverage the clinical utilization of coronary atherosclerotic plaque quantitative imaging biomarkers. Quantitative biomarkers in coronary imaging have been explored in different scenarios, such as for predicting significant hemodynamic stenosis, future plaque rupture, and monitoring disease progression or response. For instance, preliminary feasibility data comparing a quantitative CCTA (QCCTA) software with quantitative conventional ICA analysis revealed good correlations between CCTA and ICA determined stenosis (per-vessel R=0.83, p<0.01; per-patient R=0.86, p<0.01), with mean biases of −3.0±12.3% (per-vessel) and −6.2±12.4% (per-patient).[64] This study also showed improved accuracy for diagnosing lesions with stenosis ≥50% on QCCTA (95%) vs. visual CCTA analysis (87%, p=0.08). In a post hoc analysis of the NXT trial,[27] the investigators used a semi-quantitative approach to extract multiple QCCTA parameters from coronary plaques in patients with SA concurrently assessed with CCTA and ICA-FFR.[66] The investigators found that the volume of low-attenuation noncalcified plaque was a predictor of ICA-FFR-proven ischemia independent from the degree of coronary stenosis (**Figure 7**).

QCCTA was also studied in the context of prediction of future atherosclerotic plaque rupture. In a single center longitudinal study including 1,256 with suspected CAD undergoing CCTA, the investigators determined if QCCTA plaque features could predict a composite endpoint of cardiac death, myocardial infarction, unstable angina, or coronary revascularization after 90 days of the scan. Events occurred in 3.9% of the patients over a median follow-up interval of 5.7 years. The investigators found that low-attenuation plaque volume and total noncalcified

https://doi.org/10.4070/kcj.2019.0315

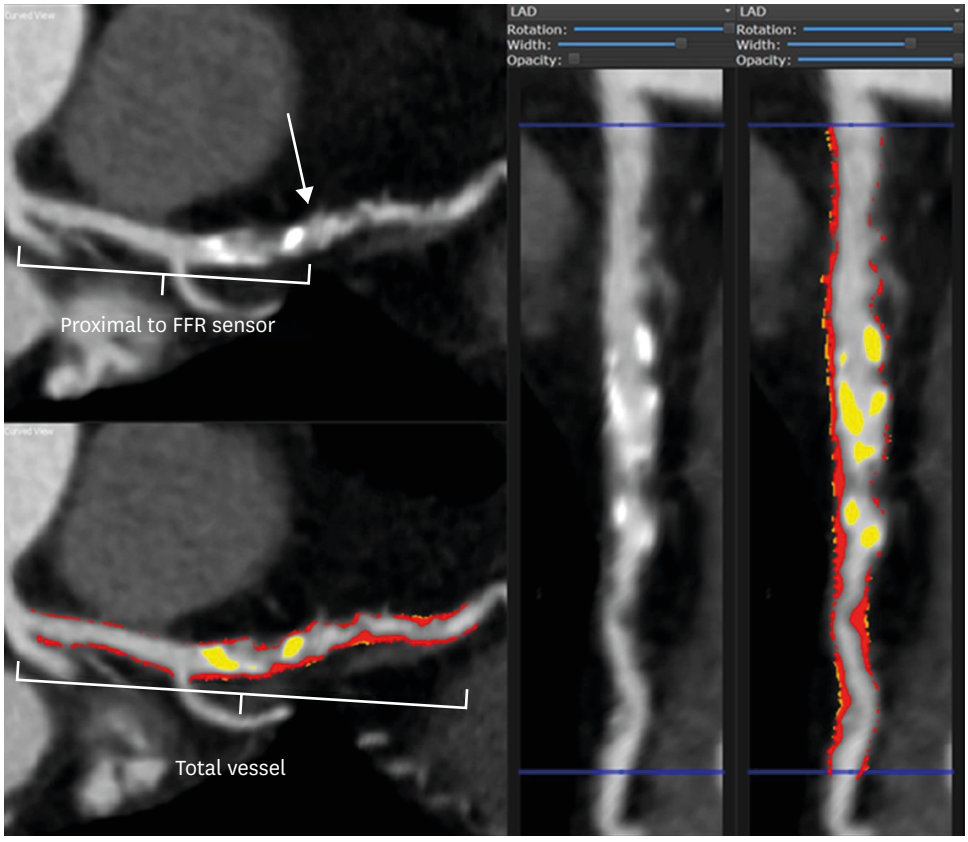

Figure 7. Quantitative plaque analysis. Left anterior descending artery. A region of interest was placed in the ascending aorta at the level of the left main coronary artery, and scan-specific thresholds for calcified plaque (yellow) and noncalcified plaque (in red) were automatically generated. Reused with permission from *J Cardiovasc Comput Tomogr* 2018;12:344-9.[66]
FFR = fractional flow reserve; LAD = left anterior descending artery.

plaque volume could predict future events after adjustment for extension of CAD, with HRs of 1.06 (95% CI, 1.01–1.1; p=0.018) and 1.10 (95% CI, 1.01–1.2, p=0.026), respectively; however, in the multivariate model, low-attenuation plaque volume was the only parameter showing incremental predictive value to coronary Agatston score, segment stenosis score, and clinical risk score.[67] In another single center case-control study including 2,748 patients, the investigators found that multiple QCCTA parameters, including volumetry of different plaque components (noncalcified, low-attenuation noncalcified, calcified, total) and quantitative stenosis, were significantly associated with cardiac mortality (p<0.025).[68] A sub-analysis of the ROMICAT II CCTA trial arm[7] has also confirmed the ability of QCCTA to identify culprit plaques in ACS using optimized CCTA-based threshold values.[69]

More recently, QCCTA has shown promise to become an objective tool for disease staging. Much information about the role of QCCTA in the assessment of the natural history of CAD has been generated from longitudinal trials or registries looking at patients undergoing serial CCTAs over long time intervals.[70] In the Progression of Atherosclerotic Plaque Determined by Computed Tomographic Angiography Imaging (PARADIGM) registry, changes in QCCTA biomarkers were used as surrogate indicators for coronary plaque progression. In this study, the investigators were able to confirm the role of diabetes mellitus as a significant risk factor for atherogenesis, especially of adverse plaque features. In another longitudinal multicenter trial including 147 patients sequentially imaged with CCTA, the investigators addressed serial

https://doi.org/10.4070/kcj.2019.0315

changes in coronary plaque burden over a minimum interval of 24 months, with focus on determining the effects of intensive therapeutic regimens to lower low-density lipoprotein cholesterol (LDL-C).[71] Overall, multiple QCCTA parameters, such as plaque volume, mean plaque burden, maximal plaque thickness, and amount of dense calcium, have significantly increased over the follow-up interval, but interestingly, the sub-analysis of patients with LDL-C <70 mg/dL revealed a significantly smaller increase in plaque volume when compared with those with LDL-C ≥70 mg/dL.

TECHNOLOGY INNOVATIONS AND EMERGING IMAGING BIOMARKERS

So far, we have explored the data behind the mainstream directions of CCTA. However, it is worthwhile to briefly mention some of the technological innovations in image acquisition, post processing, and other imaging biomarkers that have recently grown in importance, and that will likely impact how CCTAs are performed, interpreted, and clinically used in the near future.

Spectral/dual-energy CT has emerged as a new technology over a decade ago, and has become a versatile problem solver in different scenarios.[72] Some of the clinical applications involving spectral/dual-energy CT in cardiovascular imaging include amplification of intravascular contrast agent signal/attenuation, allowing for improved contrast to noise ratio in angiographic studies,[73] reduction of metallic, beam hardening and calcium blooming artifacts,[74] detection of myocardial perfusion or scarring using iodine density mapping, and characterization of atherosclerotic plaque.[75] More recently, photon-counting detector (PCD) scanners have surged as the newer iteration of spectral CT technology, with the promise to not only enhance the multi-energy/multi-material decomposition applications in CT, but also to provide high-resolution imaging of the coronaries. A preliminary study using a prototype version of a clinical PCD-CT scanner for coronary artery calcium scoring showed that the calcium to soft tissue contrast and contrast-to-noise ratios were significantly improved in PCD-CT when directly compared conventional CT images (i.e., obtained with energy integrating detectors) ($p<0.01$); in addition to better image quality, PCD-CT also performed better at lower energy levels when compared to conventional CT.[76] Another study using the same prototype demonstrated the clinical feasibility of high-resolution coronary imaging (0.25-mm-thick slices) using PCD-CT. The investigators found that stent imaging could be significantly improved by using the high-resolution PCD-CT acquisition when compared to standard dual-energy technique.[77] Future studies are still necessary to test if high-resolution imaging with PCD-CT could result in significant improvements in plaque characterization and quantification.

The future seems to be also prosperous for post processing techniques that incorporate recent developments in machine learning and artificial intelligence. As previously mentioned, although CFD-based CT-FFR has been already been established in clinical practice, newer evidence has also shown the potential for use of CFD in wall-shear stress imaging,[78] which may be a predictive element in plaque rupture.[79][80] Adverse hemodynamic plaque characteristics assessed with CFD appear to increase the capabilities of CCTA to identify culprit plaques causing ACS.[81] Even simpler methods looking at the coronary arterial geometry and tortuosity were also explored as potential biomarkers for understanding coronary atherogenesis.[82]

Radiomics is a new field in medical imaging, based on the extraction of hundreds of

https://doi.org/10.4070/kcj.2019.0315

quantitative engineered features from digital images, more extensively studied in oncologic patients, but recently proposed as an investigative tool in cardiac imaging research.[83] For example, radiomics features have recently shown promise to identify characteristics of vulnerability in coronary plaques with superiority in comparison to conventional methods.[84][85]

Machine learning encompasses a wide range of computer-based algorithms that make predictions based on massive amounts of learning data.[11] Differently from classic statistical methods, machine learning algorithms are dynamic and iterative, with predictions that are expected to improve with incremental learning data. For example, Dey et al.[86] investigated the diagnostic performance of a machine learning boosted ensemble algorithm built on top of QCCTA features from atherosclerotic plaques in 254 patients undergoing CCTA and ICA-FFR. They found that the obtained machine learning-based risk score performed with the largest AUC for detecting FFR-proven ischemia when compared to degree of stenosis, low-attenuation noncalcified plaque volume, total plaque volume, and clinical assessment (AUC of 0.84 vs. 0.76, 0.77, 0.74, 0.63, $p<0.006$, respectively).

Lastly, we should mention the discovery of secondary imaging biomarkers available on CCTA that could serve as risk factors in genesis of atherogenesis. For example, the observation of differences in epicardial fat volume and density between patients with and without established coronary atherosclerosis have suggested a potential role for epicardial fat in the genesis of the disease.[87] Epicardial fat volume obtained from calcium scoring CT was shown to improve the predictive value for obstructive CAD over traditional coronary Agatston scoring and clinical risk factors in a large observational study.[88] Perivascular epicardial fat densification has been proposed as a surrogate for inflammatory changes, and also showed incremental predictive value to standard CCTA interpretation for identifying patients at risk for cardiac death (HR, 2.06; 95% CI, 1.50–2.83; $p<0.001$).[51] There is also evidence in ACS patients that perivascular epicardial fat stranding could be an ancillary predictor of the culprit lesion.[89]

CONCLUSION

A large amount of scientific data now supports the clinical use of CCTA in the diagnosis of obstructive CAD. Current research has been shifting towards the investigation of the CCTA role in guiding patient management, identifying early predictors of ACS, and monitoring CAD progression or response to therapy. Newer methods, such as CT-FFR, have been recently translated into clinical practice, and hold the promise to provide a more specific way to determine which patients should undergo ICA. Concurrently, guidelines on structured CCTA reporting (CAD-RADS™) have already incorporated specific lexicon about plaque vulnerability. Future studies are still necessary to determine the clinical utility of quantitative plaque analysis and other quantitative imaging biomarkers, such as epicardial fat density and volume. Emerging technologies and analytical techniques such as photon-counting/spectral CT, machine learning, and radiomics will likely provide a fruitful platform for future developments in coronary imaging.

https://doi.org/10.4070/kcj.2019.0315

REFERENCES

1. Task Force MembersMontalescot G, Sechtem U, et al. 2013 ESC guidelines on the management of stable coronary artery disease: the Task Force on the management of stable coronary artery disease of the European Society of Cardiology. *Eur Heart J* 2013;34:2949-3003.
PUBMED | CROSSREF
2. Wolk MJ, Bailey SR, Doherty JU, et al. ACCF/AHA/ASE/ASNC/HFSA/HRS/SCAI/SCCT/SCMR/STS 2013 multimodality appropriate use criteria for the detection and risk assessment of stable ischemic heart disease: a report of the American College of Cardiology Foundation Appropriate Use Criteria Task Force, American Heart Association, American Society of Echocardiography, American Society of Nuclear Cardiology, Heart Failure Society of America, Heart Rhythm Society, Society for Cardiovascular Angiography and Interventions, Society of Cardiovascular Computed Tomography, Society for Cardiovascular Magnetic Resonance, and Society of Thoracic Surgeons. *J Am Coll Cardiol* 2014;63:380-406.
PUBMED | CROSSREF
3. Fordyce CB, Newby DE, Douglas PS. Diagnostic strategies for the evaluation of chest pain: clinical implications from SCOT-HEART and PROMISE. *J Am Coll Cardiol* 2016;67:843-52.
PUBMED | CROSSREF
4. SCOT-HEART investigators. CT coronary angiography in patients with suspected angina due to coronary heart disease (SCOT-HEART): an open-label, parallel-group, multicentre trial. *Lancet* 2015;385:2383-91.
PUBMED | CROSSREF
5. Douglas PS, Hoffmann U, Patel MR, et al. Outcomes of anatomical versus functional testing for coronary artery disease. *N Engl J Med* 2015;372:1291-300.
PUBMED | CROSSREF
6. Kelion AD, Nicol ED. The rationale for the primacy of coronary CT angiography in the National Institute for Health and Care Excellence (NICE) guideline (CG95) for the investigation of chest pain of recent onset. *J Cardiovasc Comput Tomogr* 2018;12:516-22.
PUBMED | CROSSREF
7. Hoffmann U, Truong QA, Schoenfeld DA, et al. Coronary CT angiography versus standard evaluation in acute chest pain. *N Engl J Med* 2012;367:299-308.
PUBMED | CROSSREF
8. Litt HI, Gatsonis C, Snyder B, et al. CT angiography for safe discharge of patients with possible acute coronary syndromes. *N Engl J Med* 2012;366:1393-403.
PUBMED | CROSSREF
9. Linde JJ, Kofoed KF, Sørgaard M, et al. Cardiac computed tomography guided treatment strategy in patients with recent acute-onset chest pain: results from the randomised, controlled trial: CArdiac cT in the treatment of acute CHest pain (CATCH). *Int J Cardiol* 2013;168:5257-62.
PUBMED | CROSSREF
10. Koo BK, Erglis A, Doh JH, et al. Diagnosis of ischemia-causing coronary stenoses by noninvasive fractional flow reserve computed from coronary computed tomographic angiograms. Results from the prospective multicenter DISCOVER-FLOW (Diagnosis of Ischemia-Causing Stenoses Obtained Via Noninvasive Fractional Flow Reserve) study. *J Am Coll Cardiol* 2011;58:1989-97.
PUBMED | CROSSREF
11. Singh G, Al'Aref SJ, Van Assen M, et al. Machine learning in cardiac CT: basic concepts and contemporary data. *J Cardiovasc Comput Tomogr* 2018;12:192-201.
PUBMED | CROSSREF
12. Pijls NH, De Bruyne B, Peels K, et al. Measurement of fractional flow reserve to assess the functional severity of coronary-artery stenoses. *N Engl J Med* 1996;334:1703-8.
PUBMED | CROSSREF
13. Fearon WF, Tonino PA, De Bruyne B, Siebert U, Pijls NH; FAME Study Investigators. Rationale and design of the Fractional Flow Reserve versus Angiography for Multivessel Evaluation (FAME) study. *Am Heart J* 2007;154:632-6.
PUBMED | CROSSREF
14. Tonino PA, De Bruyne B, Pijls NH, et al. Fractional flow reserve versus angiography for guiding percutaneous coronary intervention. *N Engl J Med* 2009;360:213-24.
PUBMED | CROSSREF
15. Pijls NH, Fearon WF, Tonino PA, et al. Fractional flow reserve versus angiography for guiding percutaneous coronary intervention in patients with multivessel coronary artery disease: 2-year follow-up of the FAME (Fractional Flow Reserve Versus Angiography for Multivessel Evaluation) study. *J Am Coll Cardiol* 2010;56:177-84.
PUBMED | CROSSREF

16. Tonino PA, Fearon WF, De Bruyne B, et al. Angiographic versus functional severity of coronary artery stenoses in the FAME study fractional flow reserve versus angiography in multivessel evaluation. *J Am Coll Cardiol* 2010;55:2816-21.
PUBMED | CROSSREF

17. Fearon WF, Bornschein B, Tonino PA, et al. Economic evaluation of fractional flow reserve-guided percutaneous coronary intervention in patients with multivessel disease. *Circulation* 2010;122:2545-50.
PUBMED | CROSSREF

18. Budoff MJ, Dowe D, Jollis JG, et al. Diagnostic performance of 64-multidetector row coronary computed tomographic angiography for evaluation of coronary artery stenosis in individuals without known coronary artery disease: results from the prospective multicenter ACCURACY (Assessment by Coronary Computed Tomographic Angiography of Individuals Undergoing Invasive Coronary Angiography) trial. *J Am Coll Cardiol* 2008;52:1724-32.
PUBMED | CROSSREF

19. Miller JM, Rochitte CE, Dewey M, et al. Diagnostic performance of coronary angiography by 64-row CT. *N Engl J Med* 2008;359:2324-36.
PUBMED | CROSSREF

20. Meijboom WB, Meijs MF, Schuijf JD, et al. Diagnostic accuracy of 64-slice computed tomography coronary angiography: a prospective, multicenter, multivendor study. *J Am Coll Cardiol* 2008;52:2135-44.
PUBMED | CROSSREF

21. Meijboom WB, Van Mieghem CA, van Pelt N, et al. Comprehensive assessment of coronary artery stenoses: computed tomography coronary angiography versus conventional coronary angiography and correlation with fractional flow reserve in patients with stable angina. *J Am Coll Cardiol* 2008;52:636-43.
PUBMED | CROSSREF

22. Taylor CA, Fonte TA, Min JK. Computational fluid dynamics applied to cardiac computed tomography for noninvasive quantification of fractional flow reserve: scientific basis. *J Am Coll Cardiol* 2013;61:2233-41.
PUBMED | CROSSREF

23. Kim HJ, Vignon-Clementel IE, Coogan JS, Figueroa CA, Jansen KE, Taylor CA. Patient-specific modeling of blood flow and pressure in human coronary arteries. *Ann Biomed Eng* 2010;38:3195-209.
PUBMED | CROSSREF

24. Kim HJ, Jansen KE, Taylor CA. Incorporating autoregulatory mechanisms of the cardiovascular system in three-dimensional finite element models of arterial blood flow. *Ann Biomed Eng* 2010;38:2314-30.
PUBMED | CROSSREF

25. Kim HJ, Vignon-Clementel IE, Figueroa CA, et al. On coupling a lumped parameter heart model and a three-dimensional finite element aorta model. *Ann Biomed Eng* 2009;37:2153-69.
PUBMED | CROSSREF

26. Min JK, Leipsic J, Pencina MJ, et al. Diagnostic accuracy of fractional flow reserve from anatomic CT angiography. *JAMA* 2012;308:1237-45.
PUBMED | CROSSREF

27. Nørgaard BL, Leipsic J, Gaur S, et al. Diagnostic performance of noninvasive fractional flow reserve derived from coronary computed tomography angiography in suspected coronary artery disease: the NXT trial (Analysis of Coronary Blood Flow Using CT Angiography: Next Steps). *J Am Coll Cardiol* 2014;63:1145-55.
PUBMED | CROSSREF

28. Coenen A, Lubbers MM, Kurata A, et al. Fractional flow reserve computed from noninvasive CT angiography data: diagnostic performance of an on-site clinician-operated computational fluid dynamics algorithm. *Radiology* 2015;274:674-83.
PUBMED | CROSSREF

29. Zhang JM, Zhong L, Luo T, et al. Simplified models of non-invasive fractional flow reserve based on CT images. *PLoS One* 2016;11:e0153070.
PUBMED | CROSSREF

30. Itu L, Rapaka S, Passerini T, et al. A machine-learning approach for computation of fractional flow reserve from coronary computed tomography. *J Appl Physiol (1985)* 2016;121:42-52.
PUBMED | CROSSREF

31. Ko BS, Cameron JD, Munnur RK, et al. Noninvasive CT-derived FFR based on structural and fluid analysis: a comparison with invasive FFR for detection of functionally significant stenosis. *JACC Cardiovasc Imaging* 2017;10:663-73.
PUBMED | CROSSREF

32. Chung JH, Lee KE, Nam CW, et al. Diagnostic performance of a Novel Method for Fractional Flow Reserve Computed from Noninvasive Computed Tomography Angiography (NOVEL-FLOW Study). *Am J Cardiol* 2017;120:362-8.
PUBMED | CROSSREF

33. Pontone G, Baggiano A, Andreini D, et al. Dynamic stress computed tomography perfusion with a whole-heart coverage scanner in addition to coronary computed tomography angiography and fractional flow reserve computed tomography derived. *JACC Cardiovasc Imaging* 2019:S1936-878X(19)30250-5.
PUBMED | CROSSREF

34. Douglas PS, Pontone G, Hlatky MA, et al. Clinical outcomes of fractional flow reserve by computed tomographic angiography-guided diagnostic strategies vs. usual care in patients with suspected coronary artery disease: the prospective longitudinal trial of FFR(CT): outcome and resource impacts study. *Eur Heart J* 2015;36:3359-67.
PUBMED | CROSSREF

35. Hlatky MA, De Bruyne B, Pontone G, et al. Quality-of-life and economic outcomes of assessing fractional flow reserve with computed tomography angiography: PLATFORM. *J Am Coll Cardiol* 2015;66:2315-23.
PUBMED | CROSSREF

36. Fairbairn TA, Nieman K, Akasaka T, et al. Real-world clinical utility and impact on clinical decision-making of coronary computed tomography angiography-derived fractional flow reserve: lessons from the ADVANCE registry. *Eur Heart J* 2018;39:3701-11.
PUBMED | CROSSREF

37. Glagov S, Weisenberg E, Zarins CK, Stankunavicius R, Kolettis GJ. Compensatory enlargement of human atherosclerotic coronary arteries. *N Engl J Med* 1987;316:1371-5.
PUBMED | CROSSREF

38. Schaar JA, Muller JE, Falk E, et al. Terminology for high-risk and vulnerable coronary artery plaques. Report of a meeting on the vulnerable plaque, June 17 and 18, 2003, Santorini, Greece. *Eur Heart J* 2004;25:1077-82.
PUBMED | CROSSREF

39. Chang HJ, Lin FY, Lee SE, et al. Coronary atherosclerotic precursors of acute coronary syndromes. *J Am Coll Cardiol* 2018;71:2511-22.
PUBMED | CROSSREF

40. Falk E, Nakano M, Bentzon JF, Finn AV, Virmani R. Update on acute coronary syndromes: the pathologists' view. *Eur Heart J* 2013;34:719-28.
PUBMED | CROSSREF

41. Hoffmann U, Moselewski F, Nieman K, et al. Noninvasive assessment of plaque morphology and composition in culprit and stable lesions in acute coronary syndrome and stable lesions in stable angina by multidetector computed tomography. *J Am Coll Cardiol* 2006;47:1655-62.
PUBMED | CROSSREF

42. Narula J, Nakano M, Virmani R, et al. Histopathologic characteristics of atherosclerotic coronary disease and implications of the findings for the invasive and noninvasive detection of vulnerable plaques. *J Am Coll Cardiol* 2013;61:1041-51.
PUBMED | CROSSREF

43. Kashiwagi M, Tanaka A, Kitabata H, et al. Feasibility of noninvasive assessment of thin-cap fibroatheroma by multidetector computed tomography. *JACC Cardiovasc Imaging* 2009;2:1412-9.
PUBMED | CROSSREF

44. Maurovich-Horvat P, Hoffmann U, Vorpahl M, Nakano M, Virmani R, Alkadhi H. The napkin-ring sign: CT signature of high-risk coronary plaques? *JACC Cardiovasc Imaging* 2010;3:440-4.
PUBMED | CROSSREF

45. Otsuka K, Fukuda S, Tanaka A, et al. Napkin-ring sign on coronary CT angiography for the prediction of acute coronary syndrome. *JACC Cardiovasc Imaging* 2013;6:448-57.
PUBMED | CROSSREF

46. Saremi F, Achenbach S. Coronary plaque characterization using CT. *AJR Am J Roentgenol* 2015;204:W249-60.
PUBMED | CROSSREF

47. Wykrzykowska J, Lehman S, Williams G, et al. Imaging of inflamed and vulnerable plaque in coronary arteries with 18F-FDG PET/CT in patients with suppression of myocardial uptake using a low-carbohydrate, high-fat preparation. *J Nucl Med* 2009;50:563-8.
PUBMED | CROSSREF

48. Alexanderson E, Slomka P, Cheng V, et al. Fusion of positron emission tomography and coronary computed tomographic angiography identifies fluorine 18 fluorodeoxyglucose uptake in the left main coronary artery soft plaque. *J Nucl Cardiol* 2008;15:841-3.
PUBMED | CROSSREF

49. Rogers IS, Nasir K, Figueroa AL, et al. Feasibility of FDG imaging of the coronary arteries: comparison between acute coronary syndrome and stable angina. *JACC Cardiovasc Imaging* 2010;3:388-97.
PUBMED | CROSSREF

50. Dweck MR, Chow MW, Joshi NV, et al. Coronary arterial 18F-sodium fluoride uptake: a novel marker of plaque biology. *J Am Coll Cardiol* 2012;59:1539-48.
PUBMED | CROSSREF

51. Oikonomou EK, Marwan M, Desai MY, et al. Non-invasive detection of coronary inflammation using computed tomography and prediction of residual cardiovascular risk (the CRISP CT study): a post-hoc analysis of prospective outcome data. *Lancet* 2018;392:929-39.
PUBMED | CROSSREF

52. Motoyama S, Kondo T, Anno H, et al. Atherosclerotic plaque characterization by 0.5-mm-slice multislice computed tomographic imaging. *Circ J* 2007;71:363-6.
PUBMED | CROSSREF

53. Motoyama S, Kondo T, Sarai M, et al. Multislice computed tomographic characteristics of coronary lesions in acute coronary syndromes. *J Am Coll Cardiol* 2007;50:319-26.
PUBMED | CROSSREF

54. Motoyama S, Sarai M, Harigaya H, et al. Computed tomographic angiography characteristics of atherosclerotic plaques subsequently resulting in acute coronary syndrome. *J Am Coll Cardiol* 2009;54:49-57.
PUBMED | CROSSREF

55. Motoyama S, Ito H, Sarai M, et al. Plaque characterization by coronary computed tomography angiography and the likelihood of acute coronary events in mid-term follow-up. *J Am Coll Cardiol* 2015;66:337-46.
PUBMED | CROSSREF

56. Puchner SB, Liu T, Mayrhofer T, et al. High-risk plaque detected on coronary CT angiography predicts acute coronary syndromes independent of significant stenosis in acute chest pain: results from the ROMICAT-II trial. *J Am Coll Cardiol* 2014;64:684-92.
PUBMED | CROSSREF

57. Ferencik M, Mayrhofer T, Bittner DO, et al. Use of high-risk coronary atherosclerotic plaque detection for risk stratification of patients with stable chest pain: a secondary analysis of the PROMISE randomized clinical trial. *JAMA Cardiol* 2018;3:144-52.
PUBMED | CROSSREF

58. Williams MC, Moss AJ, Dweck M, et al. Coronary artery plaque characteristics associated with adverse outcomes in the SCOT-HEART Study. *J Am Coll Cardiol* 2019;73:291-301.
PUBMED | CROSSREF

59. Cury RC, Abbara S, Achenbach S, et al. Coronary Artery Disease - Reporting and Data System (CAD-RADS): an expert consensus document of SCCT, ACR and NASCI: endorsed by the ACC. *JACC Cardiovasc Imaging* 2016;9:1099-113.
PUBMED | CROSSREF

60. Maroules CD, Hamilton-Craig C, Branch K, et al. Coronary artery disease reporting and data system (CAD-RADS™): Inter-observer agreement for assessment categories and modifiers. *J Cardiovasc Comput Tomogr* 2018;12:125-30.
PUBMED | CROSSREF

61. Sullivan DC, Obuchowski NA, Kessler LG, et al. Metrology standards for quantitative imaging biomarkers. *Radiology* 2015;277:813-25.
PUBMED | CROSSREF

62. Agatston AS, Janowitz WR, Hildner FJ, Zusmer NR, Viamonte M Jr, Detrano R. Quantification of coronary artery calcium using ultrafast computed tomography. *J Am Coll Cardiol* 1990;15:827-32.
PUBMED | CROSSREF

63. de Vos BD, Wolterink JM, Leiner T, de Jong PA, Lessmann N, Isgum I. Direct automatic coronary calcium scoring in cardiac and chest CT. *IEEE Trans Med Imaging* 2019;38:2127-38.
PUBMED | CROSSREF

64. Boogers MJ, Schuijf JD, Kitslaar PH, et al. Automated quantification of stenosis severity on 64-slice CT: a comparison with quantitative coronary angiography. *JACC Cardiovasc Imaging* 2010;3:699-709.
PUBMED | CROSSREF

65. Dey D, Cheng VY, Slomka PJ, et al. Automated 3-dimensional quantification of noncalcified and calcified coronary plaque from coronary CT angiography. *J Cardiovasc Comput Tomogr* 2009;3:372-82.
PUBMED | CROSSREF

66. Øvrehus KA, Gaur S, Leipsic J, et al. CT-based total vessel plaque analyses improves prediction of hemodynamic significance lesions as assessed by fractional flow reserve in patients with stable angina pectoris. *J Cardiovasc Comput Tomogr* 2018;12:344-9.
PUBMED | CROSSREF

67. Nadjiri J, Hausleiter J, Jähnichen C, et al. Incremental prognostic value of quantitative plaque assessment in coronary CT angiography during 5 years of follow up. *J Cardiovasc Comput Tomogr* 2016;10:97-104.
PUBMED | CROSSREF

68. Hell MM, Motwani M, Otaki Y, et al. Quantitative global plaque characteristics from coronary computed tomography angiography for the prediction of future cardiac mortality during long-term follow-up. *Eur Heart J Cardiovasc Imaging* 2017;18:1331-9.
PUBMED | CROSSREF

69. Bittner DO, Mayrhofer T, Puchner SB, et al. Coronary computed tomography angiography-specific definitions of high-risk plaque features improve detection of acute coronary syndrome. *Circ Cardiovasc Imaging* 2018;11:e007657.
PUBMED | CROSSREF

70. Lee SE, Chang HJ, Rizvi A, et al. Rationale and design of the Progression of AtheRosclerotic PlAque DetermIned by Computed TomoGraphic Angiography IMaging (PARADIGM) registry: a comprehensive exploration of plaque progression and its impact on clinical outcomes from a multicenter serial coronary computed tomographic angiography study. *Am Heart J* 2016;182:72-9.
PUBMED | CROSSREF

71. Shin S, Park HB, Chang HJ, et al. Impact of intensive LDL cholesterol lowering on coronary artery atherosclerosis progression: a serial CT angiography study. *JACC Cardiovasc Imaging* 2017;10:437-46.
PUBMED | CROSSREF

72. Kalisz K, Halliburton S, Abbara S, et al. Update on cardiovascular applications of multienergy CT. *Radiographics* 2017;37:1955-74.
PUBMED | CROSSREF

73. Scheske JA, O'Brien JM, Earls JP, et al. Coronary artery imaging with single-source rapid kilovolt peak-switching dual-energy CT. *Radiology* 2013;268:702-9.
PUBMED | CROSSREF

74. Bamberg F, Dierks A, Nikolaou K, Reiser MF, Becker CR, Johnson TR. Metal artifact reduction by dual energy computed tomography using monoenergetic extrapolation. *Eur Radiol* 2011;21:1424-9.
PUBMED | CROSSREF

75. Barreto M, Schoenhagen P, Nair A, et al. Potential of dual-energy computed tomography to characterize atherosclerotic plaque: ex vivo assessment of human coronary arteries in comparison to histology. *J Cardiovasc Comput Tomogr* 2008;2:234-42.
PUBMED | CROSSREF

76. Symons R, Sandfort V, Mallek M, Ulzheimer S, Pourmorteza A. Coronary artery calcium scoring with photon-counting CT: first in vivo human experience. *Int J Cardiovasc Imaging* 2019;35:733-9.
PUBMED | CROSSREF

77. Symons R, De Bruecker Y, Roosen J, et al. Quarter-millimeter spectral coronary stent imaging with photon-counting CT: initial experience. *J Cardiovasc Comput Tomogr* 2018;12:509-15.
PUBMED | CROSSREF

78. Thondapu V, Bourantas CV, Foin N, Jang IK, Serruys PW, Barlis P. Biomechanical stress in coronary atherosclerosis: emerging insights from computational modelling. *Eur Heart J* 2017;38:81-92.
PUBMED

79. Choi G, Lee JM, Kim HJ, et al. Coronary artery axial plaque stress and its relationship with lesion geometry: application of computational fluid dynamics to coronary CT angiography. *JACC Cardiovasc Imaging* 2015;8:1156-66.
PUBMED | CROSSREF

80. Han D, Starikov A, Ó Hartaigh B, et al. Relationship between endothelial wall shear stress and high-risk atherosclerotic plaque characteristics for identification of coronary lesions that cause ischemia: a direct comparison with fractional flow reserve. *J Am Heart Assoc* 2016;5:e004186.
PUBMED | CROSSREF

81. Lee JM, Choi G, Koo BK, et al. Identification of high-risk plaques destined to cause acute coronary syndrome using coronary computed tomographic angiography and computational fluid dynamics. *JACC Cardiovasc Imaging* 2019;12:1032-43.
PUBMED | CROSSREF

82. Tuncay V, Vliegenthart R, den Dekker MA, et al. Non-invasive assessment of coronary artery geometry using coronary CTA. *J Cardiovasc Comput Tomogr* 2018;12:257-60.
PUBMED | CROSSREF

83. Kolossváry M, Kellermayer M, Merkely B, Maurovich-Horvat P. Cardiac computed tomography radiomics: a comprehensive review on radiomic techniques. *J Thorac Imaging* 2018;33:26-34.
PUBMED | CROSSREF

84. Kolossváry M, Park J, Bang JI, et al. Identification of invasive and radionuclide imaging markers of coronary plaque vulnerability using radiomic analysis of coronary computed tomography angiography. *Eur Heart J Cardiovasc Imaging* 2019;20:1250-8.
PUBMED | CROSSREF

85. Kolossváry M, Karády J, Szilveszter B, et al. Radiomic features are superior to conventional quantitative computed tomographic metrics to identify coronary plaques with napkin-ring sign. *Circ Cardiovasc Imaging* 2017;10:e006843.
PUBMED | CROSSREF

86. Dey D, Gaur S, Ovrehus KA, et al. Integrated prediction of lesion-specific ischaemia from quantitative coronary CT angiography using machine learning: a multicentre study. *Eur Radiol* 2018;28:2655-64.
PUBMED | CROSSREF

87. Goeller M, Achenbach S, Marwan M, et al. Epicardial adipose tissue density and volume are related to subclinical atherosclerosis, inflammation and major adverse cardiac events in asymptomatic subjects. *J Cardiovasc Comput Tomogr* 2018;12:67-73.
PUBMED | CROSSREF

88. Zhou J, Chen Y, Zhang Y, et al. Epicardial fat volume improves the prediction of obstructive coronary artery disease above traditional risk factors and coronary calcium score. *Circ Cardiovasc Imaging* 2019;12:e008002.
PUBMED | CROSSREF

89. Hedgire S, Baliyan V, Zucker EJ, et al. Perivascular epicardial fat stranding at coronary CT angiography: a marker of acute plaque rupture and spontaneous coronary artery dissection. *Radiology* 2018;287:808-15.
PUBMED | CROSSREF

https://doi.org/10.4070/kcj.2019.0315